

TRANSVERSE IMPEDANCE AND BEAM STABILITY STUDIES FOR THE MUON COLLIDER RING* †

D. Amorim‡, F. Boattini, L. Bottura, D. Calzolari, C. Carli,
A. Lechner, E. Métral, D. Schulte, K. Skoufaris, CERN, Geneva, Switzerland
T. Pieloni, EPFL, Lausanne, Switzerland
A. Chancé, CEA-IRFU, Saclay, France

Abstract

In the framework of the International Muon Collider Collaboration, a 3 TeV center-of-mass muon collider ring is being studied, as well as a possible next stage at 10 TeV. The decay of high-energy muons represents a great challenge in terms of heat load management and radiation shielding for the superconducting magnets of the collider ring. Materials such as tungsten are being considered to shield the cold bore of the magnets from decay products. The transverse beam coupling impedance and related beam stability have been investigated in detail for several vacuum chamber designs to identify the minimum vacuum chamber radius and transverse damper properties required for stable beams.

INTRODUCTION

Circular muon colliders offer the perspective to reach high luminosity, multi-TeV center-of-mass (c.o.m) energies, overcoming the limitations from synchrotron radiation encountered with electron-positron colliders [1]. The International Muon Collider Collaboration [2, 3] has been formed to study a 3 TeV c.o.m $\mu^+ - \mu^-$ collider, with the option of a following 10 TeV c.o.m stage.

The collider ring would comprise two interaction points with instantaneous luminosities of $1.8 \times 10^{34} \text{ cm}^{-2} \text{ s}^{-1}$ for the 3 TeV and $20 \times 10^{34} \text{ cm}^{-2} \text{ s}^{-1}$ for the 10 TeV stage. To reach these high luminosities, the main challenge is to counterbalance the decay of the muon beams. With a 10 km long ring for the 10 TeV collider, the revolution period of a beam travelling at the speed of light is $33 \mu\text{s}$, much longer than the muon lifetime at rest of $\tau_0 = 2.2 \mu\text{s}$. However, thanks to relativistic time dilation, the muon lifetime in the laboratory frame τ increases with the Lorentz factor γ as $\tau = \gamma\tau_0$.

A muon production and acceleration concept, schematized in Fig. 1, was investigated by the US MAP project [4]. After the muon production, a cooling stage reduces the longitudinal and transverse emittances of the muon beam, then an acceleration stage provides fast energy increase to the muon beams to quickly increase their γ .

Once in the collider, the high-energy, high-intensity muon beams will be stored for several milliseconds. The electron

* Work funded by the Swiss Accelerator Research and Technology program (CHART).

† Funded by the European Union (EU). Views and opinions expressed are however those of the authors supported only and do not necessarily reflect those of the EU or European Research Executive Agency (REA). Neither the EU nor the REA can be held responsible for them.

‡ david.amorim@cern.ch

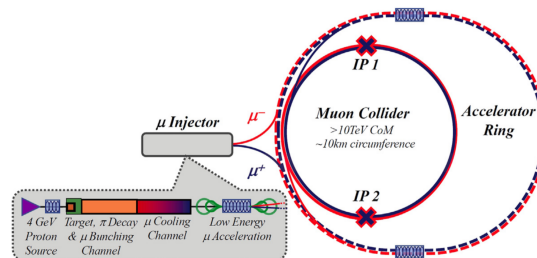


Figure 1: Proposed layout of a muon collider and its muon production and acceleration stages. Picture from Ref. [5].

and positron created by the muon decay must be intercepted to avoid excessive radiation damage and heating of the magnets superconducting coils. A first radial scheme of the 10 TeV collider magnets, schematized in Fig. 2, proposes to use a tungsten shield to intercept these decay products and remove the excess heat [6]. The innermost radius of the shield should be as small as possible to increase the available magnetic field in the center, while meeting the requirements from impedance, vacuum and optics design, among others [7, 8].

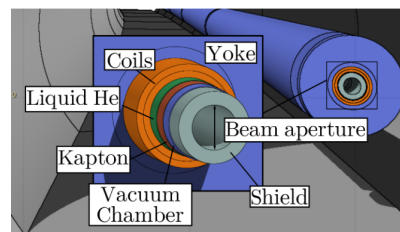


Figure 2: Radial scheme proposal for the collider magnets. The shield's function is to intercept muon decay products and protect the superconducting coils. Picture courtesy D. Calzolari [6].

The resistive-wall impedance of the 3 TeV and the 10 TeV colliders have been estimated, with scans on materials and chamber radius. With these impedance models, stability simulations were performed, scanning as well the transverse feedback strength required to stabilize the beam. This will provide the minimal radius achievable in terms of transverse coherent beam instabilities as input to the magnet design. Only the results for the 10 TeV collider will be presented here, further results on the 3 TeV collider can be found in Ref. [9].

IMPEDANCE MODEL FOR THE COLLIDER RING

The transverse beam coupling impedance model assumes a circular chamber with a length equal to the collider circumference of 10 km. Two different materials are assumed: tungsten as it is the preferred material for the shield and copper as it is a common material for beam pipe coatings and has a lower resistivity. Two different temperatures are also considered: 300 K, corresponding to a water-cooled shield and 80 K, corresponding to a cryogenically-cooled shield. The last temperature option could be a way to avoid large temperature gradients between the shield and the magnet cold bore [10]. The electrical resistivities ρ_c of these different materials are listed in Table 1 and machine parameters for the 10 TeV collider are listed in Table 2.

Table 1: Chamber Materials Resistivities

Copper at 300 K	17.9 n Ω m
Copper at 80 K	2.35 n Ω m
Tungsten at 300 K	54.4 n Ω m
Tungsten at 80 K	6.06 n Ω m

The code ImpedanceWake2D [11] is used to compute the impedance model of chambers with a radius ranging for 10 mm to 40 mm, and for the different materials listed beforehand. For these simulations, the material thickness is assumed to be infinite: the skin depth can be expressed as $\delta_{skin} = \sqrt{2\rho_c/\omega\mu_0}$, with $\omega = 2\pi f$ the angular frequency and μ_0 the free space permeability (assuming the materials have a relative permeability $\mu_r = 1$). With tungsten at 300 K and the beam revolution frequency, $f = 30$ kHz, $\delta_{skin} \approx 1$ mm is much smaller than the foreseen shield thickness of at least 20 mm. With copper at 300 K, $\delta_{skin} \approx 0.4$ mm. The infinite thickness assumed in simulations therefore holds for both a tungsten shield and a thick copper lining of the beam pipe.

Table 2: Machine Parameters for the Collider

Circumference C_0 [km]	10
Beam energy [TeV]	5
Lorentz factor	47323
Bunch intensity [10^{12} muons]	1.8
Bunch length $l\sigma_z$ [mm]	1.5
Transverse norm. emittance [μ rad]	25
Momentum compaction factor α_p	-2.0×10^{-6}
Synchrotron tune Q_s	2.33×10^{-3}
Average Twiss β_x/β_y [m]	85/51
Chromativity Q'_x/Q'_y	0/0
Number of macroparticles	20000
Number of turns simulated	5000
Number of bunches simulated	1
Transverse damper gain	2 to 500-turn + no damper

In the frequency range of interest (30 kHz to $c/\sigma_z = 200$ GHz, with σ_z the bunch length), the transverse dipolar impedance is proportional to r^{-3} , with r the chamber radius, and to $\sqrt{\rho_c}$. Therefore a small variation of the chamber radius can have a large impact on the transverse impedance as can be seen in Fig. 3, where two materials, copper and tungsten at 300 K are represented for two radii. The impedance model generated is used for transverse beam stability studies, allowing the minimum chamber radius achievable in terms of impedance to be determined.

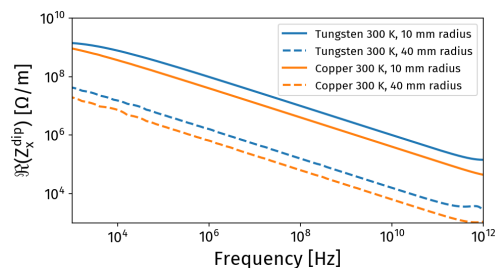


Figure 3: Transverse dipolar impedance (real part) versus frequency for circular chambers in tungsten (blue) or copper (orange) at 300 K. The two boundaries for the radius scan are represented, 10 mm (solid line) and 40 mm (dashed line).

TRANSVERSE STABILITY STUDIES WITH THE COLLIDER IMPEDANCE MODEL

Stability simulations using the impedance models described beforehand are performed with the macroparticle tracking code PyHEADTAIL [12]. The impedance is first converted to wakefields with an FFT, then a single muon beam is tracked through the transverse linear one-turn map, the longitudinal map, the wakefields and the transverse feedback system. The longitudinal map assumes that all RF cavities are lumped in one location, as the synchrotron tune remains much smaller than $1/\pi$ [13]. The transverse feedback strength is scanned from a 2-turn to 500-turn gain, and a case without feedback is also simulated. The beam is assumed to have no initial transverse offset from the injection system. Beam parameters used for the simulations are reported in Table 2.

Because of the muon decay, the bunch intensity will decrease over the storage time in the collider ring. At 5 TeV, $\gamma = 47323$ and the muon lifetime in the laboratory frame τ increases to $\tau = \gamma\tau_0 = 47323 \cdot 2.2 \mu\text{s} = 104$ ms, equivalent to 3121 turns in the 10 km long ring. A PyHEADTAIL module was implemented to account for this effect. Each turn a number of randomly selected macroparticles are removed from the simulation according to the muon beam lifetime at a given energy. This is illustrated in Fig. 4 which compares the number of macroparticles in a bunch with the turn number against the decay law $N(t) = N_0 \exp(-t/\tau)$, where N_0 is the initial number of particles in the bunch and $N(t)$ the number of particles at time t .

The transverse emittance of the bunch is monitored and saved at each turn, allowing the growth ratio $\varepsilon_t/\varepsilon_0$ to be com-

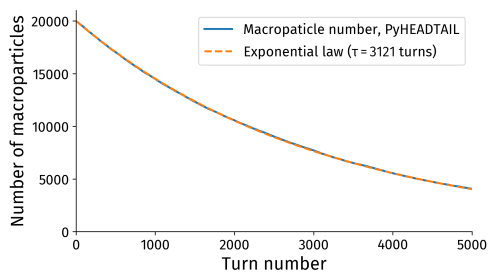


Figure 4: Intensity decay over time for a bunch of 20000 macro-particles carrying a total charge of 1.8×10^{12} muons at turn 0. The PyHEADTAIL implementation is compared to the exponential decay law with $\tau = 3121$ turns.

puted, where ε_t is the emittance at time t and $\varepsilon_0 = 25 \mu\text{m rad}$ is the initial transverse emittance. Figure 5 illustrates the results obtained for chambers in copper at 300 K. The growth ratio after 2000 turns is computed for each chamber radius (horizontal axis) and transverse feedback gain (vertical axis). When this ratio is equal to one (yellow color), the beam was stable in simulation. If the growth ratio is larger than 1.2, the beam is considered unstable.

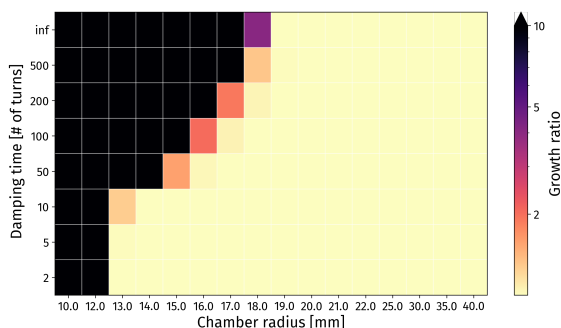


Figure 5: Emittance growth ratio versus beam chamber radius and damping time. An infinite damping time corresponds to simulations without transverse feedback. The emittance ratio is computed after 2000 turns of simulation.

This analysis is repeated for the different materials, chamber radii and transverse feedback gains. The results are summarized in Fig. 6 which shows the minimum radius achievable for each damping time and material (solid lines). Simulations without the muon decay effect were also performed (dashed lines) to show the benefit of the intensity reduction caused by muon decay on the minimum radius achievable.

Low-resistivity materials such as copper at 300 K or cryogenically-cooled materials allow tighter radii to be reached for a given transverse feedback setting. A chamber radius below 20 mm can be achieved with copper at 300 K as the innermost layer of the vacuum chamber, and with feedback settings in the 100-turn range. Using directly the tungsten shield as the innermost layer would however require a strong damper to reach chamber radii below 20 mm. Cryogenically-cooled materials offer the best performance in terms of impedance but their implementation as a shielding

material would be more difficult and the required cooling power larger than a solution at 300 K.

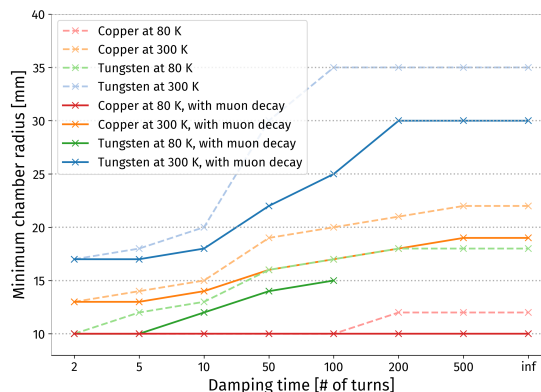


Figure 6: Minimum chamber radius allowed to keep emittance growth below 20% after 300 turns versus damping time. Radius below 10 mm were not studied.

CONCLUSION

The muon decay in the collider ring requires a heavy shield surrounding the beam to intercept the decay products before they reach the superconducting magnet coils. To reach the maximum magnetic field in the center of the vacuum chamber while keeping a reasonable magnet size, the magnet aperture must be as small as possible. Transverse beam instabilities become a concern as the vacuum chamber radius decreases, and have therefore been studied for the 10 TeV collider.

Impedance models assuming copper or tungsten chambers at 300 K or 80 K were created for a range of chamber radii between 10 mm and 40 mm. With these impedance models, tracking simulations were performed with PyHEADTAIL to find the stability limits versus the chamber radius and the transverse feedback gain. The muon decay effect was also implemented in the tracking code, showing the beneficial effect on transverse beam stability of the beam intensity loss over time.

A chamber radius below 20 mm requires using either lower resistivity materials such as copper at 300 K or cryogenically-cooled materials, or a strong transverse feedback setting if tungsten is directly used as the innermost material for the vacuum chamber.

A refined impedance model for the collider vacuum chamber is now being developed, assuming a copper coating on tungsten to better reflect the design constraints. Additional mitigation measures such as a slightly positive chromaticity could also be considered. The two beam impedance and stability, as well as the effect of an initial transverse offset created by the injection process will also be studied in the future.

ACKNOWLEDGEMENTS

The authors would like to thank Scott Berg and Mark Palmer for the fruitful discussions.

REFERENCES

- [1] M. Boscolo, J.-P. Delahaye, and M. Palmer, “The future prospects of muon colliders and neutrino factories,” *Reviews of Accelerator Science and Technology*, vol. 10, no. 01, pp. 189–214, 2019. doi:10.1142/S179362681930010X
- [2] D. Schulte, “The International Muon Collider Collaboration,” in *Proc. IPAC’21*, Campinas, SP, Brazil, 2021, paper THPAB017, pp. 3792–3795. doi:10.18429/JACoW-IPAC2021-THPAB017
- [3] Muon Collider Collaboration. <https://muoncollider.web.cern.ch>
- [4] M. A. Palmer, “An Overview of the US Muon Accelerator Program,” in *Proc. COOL’13*, Murren, Switzerland, 2013, paper MOAM2HA02, pp. 16–20.
- [5] K. Long, D. Lucchesi, M. Palmer, N. Pastrone, D. Schulte, and V. Shiltsev, “Muon Colliders: Opening New Horizons for Particle Physics,” *Nature Phys.*, vol. 17, pp. 289–292, 2021. doi:10.1038/s41567-020-01130-x
- [6] D. Calzolari *et al.*, “Radiation Load Studies for Superconducting Dipole Magnets in a 10 TeV Muon Collider,” in *Proc. IPAC’22*, Bangkok, Thailand, 2022, paper WEPOST001, pp. 1671–1674. doi:10.18429/JACoW-IPAC2022-WEPOST001
- [7] K. Skoufaris, C. Carli, and D. Schulte, “10 TeV Center of Mass Energy Muon Collider,” in *Proc. IPAC’22*, Bangkok, Thailand, 2022, paper MOPOTK031, pp. 515–518. doi:10.18429/JACoW-IPAC2022-MOPOTK031
- [8] K. Skoufaris, C. Carli, and D. Schulte, “First Design of a 10 TeV Centre of Mass Energy Muon Collider,” in *Proc. IPAC’23*, Venice, Italy, 2023, paper MOPL064.
- [9] D. Amorim, “3 TeV collider transverse impedance and stability,” in *IMCC Annual meeting 2022*, Geneva, Switzerland, 2022. <https://indico.cern.ch/event/1175126/contributions/5025354>
- [10] N. V. Mokhov, V. V. Kashikhin, S. I. Striganov, I. S. Tropin, and A. V. Zlobin, “The Higgs Factory Muon Collider Superconducting Magnets and Their Protection Against Beam Decay Radiation,” *JINST*, vol. 13, no. 10, P10024, 2018. doi:10.1088/1748-0221/13/10/P10024
- [11] ImpedanceWake2D. https://abpcomputing.web.cern.ch/codes/codes_pages/ImpedanceWake2D
- [12] PyHEADTAIL. <https://github.com/PyCOMPLETE/PyHEADTAIL>
- [13] T. Suzuki, “Equations of motion and Hamiltonian for synchrotron oscillations and synchro-betaatron coupling,” KEK, Tsukuba, Japan, Tech. Rep. KEK-REPORT-96-10, 1996.